Multicarrier DS-SS for GPS Pseudolites: Code-Acquisition Performance in the Presence of Data Modulation

K. R. Shankar kumar and **A. Chockalingam**

Department of Electrical Communication Engineering
Indian Institute of Science, Bangalore 560012, INDIA

Abstract

In this paper, we analyze the code acquisition performance of a multicarrier direct-sequence spread spectrum (DS-SS) system in the presence of data modulation (i.e., no pilot) on multipath Rayleigh fading channels. The motivation of this analysis arises from the possibility of beneficially using multicarrier DS-SS in global positioning system (GPS) *pseudolites*, where unmodulated pilot is not available. We consider equal gain combining (EGC) and selection combining (SC) of subcarrier correlator outputs for each timing hypothesis. We evaluate probability of incorrect decision and mean acquisition time performance of the multicarrier DS-SS code acquisition scheme. We show that significant reduction in the mean acquisition time (MAT) can be achieved using the multicarrier DS-SS approach for GPS pseudolites.

Keywords – Multicarrier systems, DS-SS, code acquisition, GPS pseudolites.

1 Introduction

Multicarrier code division multiple access (MC-CDMA) using direct-sequence spread spectrum (DS-SS) has drawn significant research attention recently due to its advantages including robustness in multipath fading, resistance to narrowband interference, and non-contiguous bandwidth operation [1],[2]. Fast code acquisition is an important performance requirement in DS-SS systems. In cellular DS-CDMA systems, pilot spreading code signals are typically sent without any data modulation on them (i.e., all 1's data) to enable fast code acquisition. However, in DS-SS systems like global positioning system (GPS), the spread signal is always data modulated. The GPS transmitter spreads a 50 bps data stream using a 1023 chip Gold sequence at a chip rate of 1 Mcps. Hence, the code acquisition must be performed in the presence of data modulation. Cheng, in [3], has studied the loss in acquisition performance due to data modulation in parallel acquisition schemes, assuming an AWGN channel.

Our focus in this paper is the analysis of the code-acquisition performance of a multicarrier DS-SS system with data modulation (i.e., no pilot) on multipath Rayleigh fading channels. The motivation of this analysis arises from the possibility of beneficially using multicarrier DS-SS in GPS *pseudolites*. Pseudolites are small, ground-based transmitters that emulate the signal structure of the GPS satellite transmitters, with an intent to augment the GPS system performance in terms of enhanced location accuracy [4],[5]. Pseudolite transmissions are envisaged to provide better than one meter accuracy for various applications including indoor location, aircraft landing, mobile phones, etc. A main concern with the ground-based pseudolite transmission is the effect of multipath fading. We note that the use of multicarrier DS-SS for pseudolite transmissions can be beneficial in combating the effects of a multipath fading. Several performance and system complexity questions arise in this context. In this paper, we address one such performance question; that is, analyze the code-acquisition performance of multicarrier DS-SS with data modulation (i.e., no pilot) on multipath Rayleigh fading channels. We evaluate probability of incorrect decision and mean acquisition time performance of the multicarrier DS-SS code acquisition scheme. We show that significant reduction in the mean acquisition time (MAT) can be achieved using the multicarrier DS-SS approach for GPS pseudolites.

The rest of the paper is organized as follows. In Section 2, the system model including the multicarrier DS-SS transmitter, channel model and the code acquisition system are presented. Section 3 presents the mean acquisition time performance analysis. Numerical results and discussions are presented in Section 4. Conclusions are presented in Section 5.

2 System Model

Consider a multicarrier system where the available bandwidth W is divided into M equal-width, disjoint frequency bands, such that the bandwidth of each sub-band is given by $W_m = W/M$, $m = 1, 2, ..., M$. Each sub-band carries a narrowband DS-SS waveform of bandwidth given by $W_m = (1 + a)/MT_c$, $m = 1, 2, ..., M$, where $0 < a \leq 1$ is the measure of excess bandwidth of the system, and MT_c is the chip duration of the multicarrier DS-SS system.

We consider the multicarrier DS-SS transmitter shown

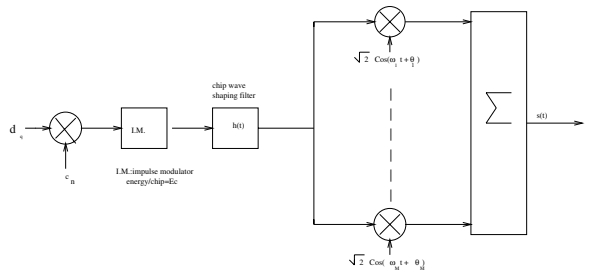

Figure 1: Multicarrier DS-SS transmitter.

in Fig. 1. The transmitted signal is given by

$$s(t) = \sqrt{2E_c} \sum_{n=-\infty}^{\infty} d_q c_n h(t-nMT_c) \sum_{m=1}^{M} \cos(\omega_m t+\theta_m), \quad (1)$$

where $\{d_q\}$, $q = \lfloor n/N \rfloor$ represents the transmitted data, N is the number of chips per data bit, $\{c_n\}$ represents the spreading sequence, $h(t)$ is the impulse response of the chip wave shaping filter, M represents the number of sub-bands each of width W/M Hz, and ω_m and θ_m are the m^{th} subcarrier's frequency and phase, respectively. In pilot-aided acquisition schemes, $\{d_q\}$ will be all 1's data, whereas in GPS like transmissions, $\{d_q\}$ will correspond to the information data bits. In this paper, we consider two cases; $\{d_q\}$ being *random data* (RD) stream and *alternate data* (AD) stream (i.e., 10101010... stream, which represents the worst case data transitions scenario). The received signal, $r(t)$, is given by

$$r(t) = \sqrt{2E_c} \sum_{n=-\infty}^{\infty} d_{\lfloor (n+D)/N \rfloor} c_{n+D} \quad (2)$$

$$\cdot h(t - nMT_c - \epsilon) \sum_{m=1}^{M} \alpha_m \cos(\omega_m t + \theta'_m) + n(t),$$

where D is the phase of the code chip sequence, ϵ is the unknown time delay given by $\epsilon = DMT_c + \tau$ and τ is assumed to be uniformly distributed over $[0, MT_c)$, α_m represents the fade amplitude on the m^{th} subcarrier which is a Rayleigh random variable with $E[\alpha_m^2] = 1$, ϕ_m is the channel introduced random phase on the m^{th} subcarrier which is a uniform random variable over $[0, 2\pi)$, $\theta'_m = \theta_m + \phi_m$, and $n(t)$ is the AWGN with a psd of $\eta_0/2$.

Fig. 2 shows the code-acquisition scheme at the multicarrier DS-SS receiver. There are M noncoherent correlators, one on each of the M subcarrier branches. If U_1 is the number of hypothesis to be tested in a single-carrier system ($M = 1$), then the number of hypothesis to be tested in a multicarrier system ($M > 1$) will be $U = U_1/M$ (since one chip duration in a multicarrier system is M times that of a single-carrier system). For each timing hypothesis that is tested, these correlators generate M output statistics $z_m^{(j)}$, where $z_m^{(j)}$ is the m^{th} correlator output for the j^{th} hypothesis, $m = 1, 2, ..., M$ and $j = 1, 2, ...U$. We consider two ways of combining the M correlator outputs for each timing hypothesis; equal gain combining (EGC) and selection combining (SC). In EGC, the combiner output statistic for the j^{th} hypothesis is given by $Z^{(j)} = \sum_{m=1}^{M} z_m^{(j)}$. In SC, the maximum

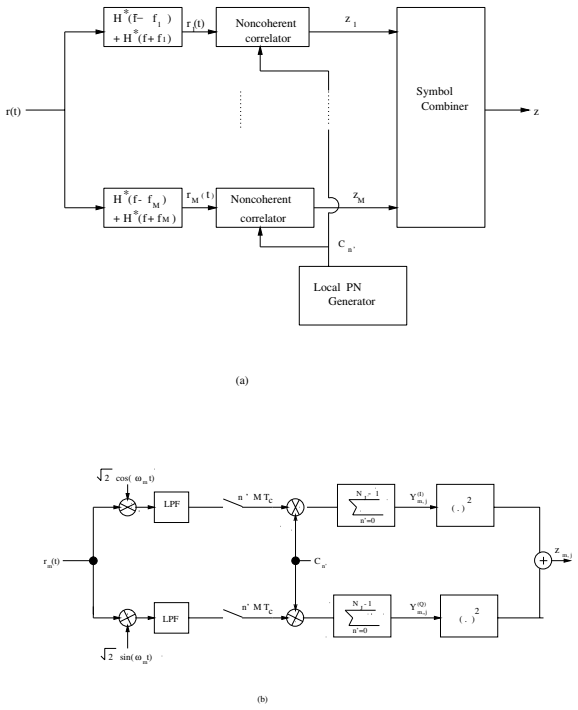

Figure 2: Block diagrams of a) multicarrier DS-SS code-acquisition scheme, and b) *m*th branch noncoherent correlator.

among the M correlator outputs is taken as the combiner output, i.e., $Z^{(j)} = \max(z_1^{(j)}, z_2^{(j)}, ..., z_M^{(j)})$. The hypothesis for which $Z^{(j)}$, $j = 1, 2, ...U$ is maximum is declared as the correct timing hypothesis.

3 Performance Analysis

In this section, we present the analysis of the performance of the code-acquisition scheme described above. Specifically, we derive the expressions for the probability of incorrect decision, which is used in the computation of the mean acquisition time. We define the probability of incorrect decision, P_e, as the probability that the maximum $Z^{(j)}$ does not correspond to the correct timing hypothesis. We take the integration time for each hypothesis in the noncoherent correlator to be one data bit duration. The one bit integration period is divided into $J = MJ_1$ subintervals, where J_1 is the number of subintervals when $M = 1$. Since we take the total integration time to be one data bit duration, only one of the J subintervals will encounter data transition and hence signal loss. We model this signal loss due to data transitions by a uniform r.v β, and obtain the correlator output statistics (mean and variance) for each subinterval, conditioned on β and H_k, $k = 0, 1$, where H_0 and H_1 correspond to the incorrect and correct hypothesis, respectively. The output of the m^{th} correlator branch, $z_m^{(j)}$, is obtained by summing up the output from of all the J subintervals. We then obtain the pdf of the combined signal output, $Z^{(j)}$, by using the characteristic function of $z_m^{(j)}$, and applying Cauchy residue theorem. From the pdf of the combined signal output, we obtain the probability of incorrect decision, P_e.

3.1 Correlator Output Statistics

As is [6], to keep the analysis tractable, α_m and ϕ_m are assumed to be constant and independent in each of the subintervals of the mth branch noncoherent correlator. So, we have the transfer function of the jth subinterval for the mth subcarrier to be $\alpha_{m,j}e^{j\phi_{m,j}}$, where the $\alpha_{m,j}$ and the $\phi_{m,j}$ are independent and identically distributed (i.i.d) Rayleigh random variables with a unit second moment, and i.i.d. uniform random variables over $[0, 2\pi)$, respectively.

Now, we have the inphase and quadrature components, obtained by integrating over N_J chips in the jth subinterval of the mth noncoherent correlator to be

$$Y_{m,j}^{(I)} = \sqrt{\frac{E_c}{M}}\alpha_{m,j}S(\epsilon)\cos(\theta'_{m,j}) + N_{Y_{m,j}}^{(I)}, \quad (3)$$

$$Y_{m,j}^{(Q)} = \sqrt{\frac{E_c}{M}}\alpha_{m,j}S(\epsilon)\cos(\theta'_{m,j}) + N_{Y_{m,j}}^{(Q)}, \quad (4)$$

where

$$S(\epsilon) = \sum_{n'=0}^{N_J-1}\sum_{n=-\infty}^{\infty} d_{\lfloor (n+D)/N\rfloor}c_{n+D}c_{n'} \cdot x[(n'-n)MT_c - \epsilon], \quad (5)$$

$$N_{Y_{m,j}}^{(I)} = \sum_{n'=0}^{N_J-1} c_{n'}[\text{Lpf}\{n'_m(t)\sqrt{2}\cos(\omega_m t)\}_{t=n'MT_c}], \quad (6)$$

$$N_{Y_{m,j}}^{(Q)} = \sum_{n'=0}^{N_J-1} c_{n'}[\text{Lpf}\{n'_m(t)\sqrt{2}\sin(\omega_m t)\}_{t=n'MT_c}]. \quad (7)$$

In Eqns. (6) and (7), the term $n'_m(t)$ is $n(t)$ after passing through the mth bandpass filter, and Lpf represents a low-pass filtering operation after which double frequency terms can be ignored. Note that $N_{Y_{m,j}}^{(I)}$ and $N_{Y_{m,j}}^{(Q)}$ are Gaussian by assumption [1]. The variances of $N_{Y_{m,j}}^{(I)}$ and $N_{Y_{m,j}}^{(Q)}$ are given by $\sigma_{m,j}^2 \triangleq var\{N_{Y_{m,j}}^{(I)}\} = var\{N_{Y_{m,j}}^{(Q)}\} = N_J\eta_0/2$.

It is assumed that $S(\epsilon)$ has two values: μ_1 under the condition of H_1 and μ_0 under the condition of H_0. Since $X(f)$ satisfies the Nyquist criterion, we have $x[(n'-n)MT_c] = 0$ for $n' \neq n$, μ_1 and μ_0 are given by $\pm\beta N$ and $\sum_{n'=0}^{N_J-1} d_{\lfloor (n'+D)/N\rfloor}c_{n'}c_{n'+D}$, respectively. In this, β is a random variable, uniformly distributed between [0,1], which accounts for the signal loss due to data modulation.

The output due to the jth subinterval in the noncoherent correlator of the mth branch is given by $z_{m,j} = \{Y_{m,j}^{(I)}\}^2 + \{Y_{m,j}^{(Q)}\}^2$. For given $\alpha_{m,j}, \theta'_{m,j}$ and μ_k, we have $Y_{m,j}^{(I)}$ and $Y_{m,j}^{(Q)}$ are independent Gaussian random variables with variance $\sigma_{m,j}^2$ and means $\sqrt{\frac{E_c}{M}}\alpha_{m,j}\mu_k\cos(\theta'_{m,j})$ and $\sqrt{\frac{E_c}{M}}\alpha_m\mu_k\sin(\theta'_{m,j})$, respectively. Therefore, the conditional probability density function of $z_{m,j}$, conditioned on $\alpha_{m,j}$ and $H_k(k = 0, 1)$, is a non-central χ^2 random variable with two degrees of freedom. After removing the conditioning on $\theta'_{i,j}$, we get

$$p_{z_{m,j}|\alpha_{m,j},H_k,\beta}(z_{m,j}|\alpha_{m,j}, H_k, \beta) = \frac{1}{2\sigma_{m,j}^2} I_0\left(\frac{\sqrt{\frac{E_c}{M}z_m}}{\sigma_{m,j}^2}\mu_k\alpha_{m,j}\right) \cdot\exp\left(-\frac{z_m + \frac{E_c}{M}\mu_k^2\alpha_{m,j}^2}{2\sigma_{m,j}^2}\right), \quad (8)$$

where $I_0(x)$ is the zeroth modified Bessel function of the first kind. After removing the conditioning on $\alpha_{m,j}$, we get

$$p_{z_{m,j}|H_k,\beta}(z_{m,j}|H_k, \beta) = \frac{1}{2v_{m,j,k}}\exp\Big(-\frac{z_{m,j}}{2v_{m,j,k}}\Big), \quad (9)$$

where $v_{m,j,k} = \sigma_{m,j}^2 + m_k^2/2$ and $m_k = \sqrt{\frac{E_c}{M}\mu_k^2}$.

3.2 Probability of Incorrect Decision

As in [6], to keep the analysis tractable, we assume that $\mu_0 = 0$. This means that the shifts of the spreading sequences are orthogonal irrespective of the data modulation, and, therefore, the noise out of the parallel branches are uncorrelated. The probability of incorrect decision (i.e., the probability that the maximum $Z^{(j)}$ does not correspond to the correct timing hypothesis) is given by

$$P_e = 1 - \int_0^\infty p_{z|H_1,\beta}(z|H_1, \beta) \cdot\left[\int_0^z p_{z|H_0,\beta}(y|H_0, \beta)dy\right]^{U-1} dz, \quad (10)$$

where U is the number of hypotheses to be tested and $p_{z|H_1,\beta}(z|H_1, \beta)$ is the conditional pdf of the symbol combiner output z conditioned on H_k and β. We consider two symbol combining methods namely, equal gain combining (EGC) and selection combining (SC).

A. *Equal Gain Combining*

The output of the equal gain combiner is given by

$$z = \sum_{m=1}^{M} z_m, \quad (11)$$

where z_m, the output of the mth branch noncoherent correlator, is given by

$$z_m = \sum_{j=1}^{J} z_{m,j}. \quad (12)$$

In our analysis, we have taken the total integration time to be one data bit. In that case, only one of the subinterval in any of the mth branch noncoherent correlator will encounter data transition and we will assume that to be the first subinterval itself. Then, the first subinterval that encounters data transition will have $\mu_1 = \pm\beta N_J$ and the

rest of the $J-1$ subintervals in the mth branch noncoherent correlator will have $\mu_1 = \pm N_J$.

In every z_m, all the $z_{m,j}$'s are independent random variables. So, we have

$$p_{z_m|H_k,\beta}(z_m|H_k,\beta) = \frac{1}{2\pi j}\oint \exp(-sz_m)\prod_{j=1}^{J}\Phi_{z_{m,j}|H_k,\beta}(s)ds, \tag{13}$$

where $\Phi_{z_{m,j}|H_k,\beta}$ is the characteristic function of of $z_{m,j}$, conditioned on H_k and β, and is given as

$$\begin{aligned}\Phi_{z_{m,j}|H_k,\beta}(s) &= \int_0^\infty \exp(sz_{m,j})p_{z_{m,j}|H_k,\beta}(z_{m,j}|H_k,\beta)dz_{m,j} \\ &= \frac{1}{1-2v_{m,j,k}s}.\end{aligned} \tag{14}$$

To obtain $\Phi_{z_{m,j}|H_k,\beta}(s)$ for the first subinterval in the mth branch that encounters data transition, we will have to replace $v_{m,1,1}$ in the Eqn. (14), by $\sigma^2_{m,j} + (\beta N_J)^2/2$ and $\sigma^2_{m,j} + ((\beta+1)N_J)^2/8$ for AD and RD cases respectively, and $v_{m,1,0} = \sigma^2_{1,1}$ for both AD and RD.

Since the z_m's are independent random variables, the pdf of z given H_k and β is

$$p_{z|H_k,\beta}(z|H_k,\beta) = \frac{1}{2\pi j}\oint \exp(-sz)\prod_{m=1}^{M}\Phi_{z_m|H_k,\beta}(s)ds. \tag{15}$$

When H_1 is true, we will have

$$p_{z|H_1,\beta}(z|H_1,\beta) = \frac{1}{2\pi j}\oint \frac{\exp(-sz)}{(1-2v_{m,2,1}s)^{MJ-M}(1-2v_{m,1,1}s)^{M}}ds. \tag{16}$$

From the Cauchy residue theorem [8], Eqn. (16) equals

$$\begin{aligned}p_{z|H_1,\beta}(z|H_1,\beta) = &\frac{f_1(\frac{1}{2v_{m,2,1}},z)}{(2v_{m,2,1})^{MJ-M}(MJ-M-1)!} \\ &+\frac{f_2(\frac{1}{2v_{m,1,1}},z)}{(M-1)!(2v_{m,1,1})^{M}},\end{aligned} \tag{17}$$

where

$$f_1(s,z) = \frac{\partial^{MJ-M-1}}{\partial s^{MJ-M-1}}\left(\frac{(-1)^{MJ-M-1}\exp(-sz)}{(1-2v_{m,1,1}s)^{M}}\right), \tag{18}$$

$$f_2(s,z) = \frac{\partial^{M-1}}{\partial s^{M-1}}\left(\frac{(-1)^{M}\exp(-sz)}{(1-2v_{m,2,1}s)^{MJ-M}}\right). \tag{19}$$

When H_0 is true, we will have $v_{m,j,0} = \sigma^2_{1,1}$. So, we will obtain

$$\begin{aligned}p_{z|H_0,\beta}(z|H_0,\beta) &= p_{z|H_0}(z|H_0), \\ &= \frac{1}{2\pi j}\oint \frac{\exp(-sz)}{(1-2\sigma^2_{1,1}s)^{MJ}}ds.\end{aligned} \tag{20}$$

Again, from Cauchy residue theorem [8], we get

$$p_{z|H_0,\beta}(z|H_0,\beta) = \frac{z^{MJ-1}\exp(-\frac{z}{2\sigma^2_{1,1}})}{(2\sigma^2_{1,1})^{MJ}(MJ-1)!}. \tag{21}$$

The integration of Eqn. (21) gives [9]

$$\int_0^z p_{z|H_0,\beta}(y|H_0,\beta) = 1 - \sum_{k=0}^{MJ-1}\left(\frac{z}{2\sigma^2_{1,1}}\right)^k\frac{\exp(-\frac{z}{2\sigma^2_{1,1}})}{k!}. \tag{22}$$

The integration of Eqn. (10) is done numerically.

B. *Selection Combining*

The output of the selection combiner is given by

$$z = \max(z_1, z_2..., z_M), \tag{23}$$

where $z_m, m = 1, 2, ..., M$, is given by Eqn. (12). The conditional pdf of z conditioned on H_k and β is given by

$$p_{z|H_k}(z|H_k) = \frac{\partial\, pr\{z_1 \le z, z_2 \le z, ..., z_M \le z|H_k,\beta\}}{\partial z} \tag{24}$$

The conditional pdf of $z_m, m = 1, 2, ..., M$, given H_k and β is obtained from Eqn. (17) and Eqn. (21) by replacing M by $M = 1$. The evaluation of Eqn. (24) and Eqn. (10) is done numerically.

3.3 Mean Acquisition Time

From the probability of incorrect decision, the mean acquisition time for the acquisition procedure is given by [10]

$$\overline{T_a} = UT_i + (UT_i + T_P)\frac{P_e}{(1-P_e)}, \tag{25}$$

where U is the number of hypotheses to be tested, T_i is the noncoherent correlator integration time for each hypothesis (which is taken to be 1 bit duration) and T_P is the penalty time incurred in case of a incorrect decision.

4 Numerical Results

In Figs. 3, 4 and 5, we plot the probability of incorrect decision, P_e, for both single-carrier ($M = 1$) as well as multicarrier ($M = 2, 4$) DS-SS, for no data (ND) modulation (Fig. 3), alternate data (AD) modulation (Fig. 4), and random data (RD) modulation (Fig. 5). Results for both equal gain combining (EGC) and selection combining (SC) are given for the multicarrier scheme. The number of subintervals, J_1, for the single-carrier system is taken to be 4 (so that the number of subintervals in the multicarrier system, $J = MJ_1$) and the value of β is taken to be 0.5. As in GPS, the chip rate is 1 Mcps, the data rate is 50 bps (i.e., 1 bit time = 20 msec), the number of chips per bit $N_1 = 20460$, and the number of hypotheses to be tested $U_1 = 1023$. It is observed that the multicarrier system (both EGC and SC) provides much lower probability of incorrect decision compared to the single-carrier system. Also, as the number of subcarriers M is increased, P_e decreases. For a given M, EGC performs better than SC.

In Figs. 6 and 7, we plot the mean acquisition time (MAT) as a function of the number of subintervals, J_1, for both single-carrier ($M = 1$) as well as multicarrier ($M = 2, 4$) DS-SS, for alternate data (AD) modulation (Fig. 6) and random data (RD) modulation (Fig. 7) at an $E_b/\eta_0 = MNE_c/\eta_0$ of 22 dB. We have taken $T_i = 20$ msec (which is equal to one bit duration in GPS) and $T_P = 1000T_i$ (i.e., 20 secs). Since U and P_e for multicarrier DS-SS are much smaller than those of a single-carrier system, significant reduction in MAT is achieved

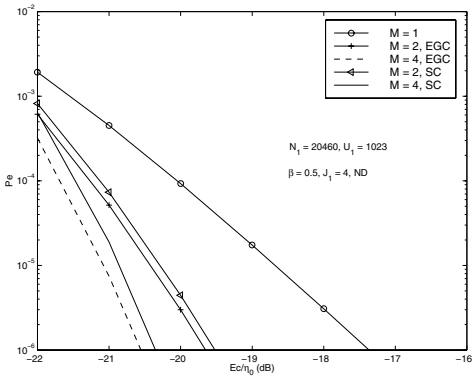

Figure 3: Probability of incorrect decision, P_e, versus E_c/η_0 performance of single-carrier ($M = 1$) and multicarrier ($M = 2, 4$) DS-SS with EGC and SC. No data modulation (ND).

using the multicarrier approach. For the considered case of large SNR ($E_b/\eta_0 = 22$ dB), it is observed that, as the number of subintervals is increased the MAT for both the AD and RD cases decreases due to more number of independent observations being combined.

5 Conclusion

Motivated by the possibility of using multicarrier DS-SS in GPS pseudolites, we analyzed the probability of incorrect decision and mean acquisition time performance of a multicarrier DS-SS system in the presence of data modulation (i.e., no pilot) on multipath Rayleigh fading channels. We considered equal gain combining and selection combining of subcarrier correlator outputs for each timing hypothesis. We showed that significant reduction in the mean acquisition time can be achieved using the multicarrier DS-SS approach for GPS pseudolites.

References

[1] S. Kondo and L. B. Milstein, "Performance of multicarrier DS CDMA systems," *IEEE Trans. Commun.,* vol. 44, no. 2, pp. 238-246, February 1996.

[2] E. A. Sourour and M. Nakagawa, "Performance of orthogonal multicarrier CDMA in a multipath fading channel," *IEEE Trans. Commun.,* vol. 44, no. 3, pp. 356-367, March 1996.

[3] U. Cheng, "Performance of a class of parallel spread-spectrum code acquisition schemes in the presence of data modulation," *IEEE Trans. Commun.,* vol. 36, no. 5, pp. 596-604, May 1988.

[4] H. S. Cobb, *GPS Pseudolites: Theory, Design and Applications,* Ph.D Thesis, Stanford Univ., September 1997.

[5] J. M. Stone, E. A. LeMaster, J. D. Powel, and S. Rock, "GPS pseudolite transceivers and their applications," *Proc. ION NTM'99,* January 1999. http://arl.stanford.edu/~ rover/info.html#Papers

[6] D. Lee, L. B. Milstein, and H. Lee, "Analysis of a multicarrier DS-CDMA code-acquisition system," *IEEE Trans. Commun.,* vol. 47, no. 8, pp. 1233-1244, August 1999.

[7] M. K. Simon *et al., Spread Spectrum Communications.* vol. 3. Rockville, MD: Computer Science, 1985.

[8] Z. Nehari, *Introduction to Complex Analysis*, Boston, MA: Allyn and Bacon, 1961.

[9] J. G. Proakis, *Digital Communications*, McGraw-Hill, 1995.

[10] R. L. Peterson, R. E. Ziemer, and D. E. Borth, *Introduction to spread-spectrum communications*, Prentice Hall, 1995.

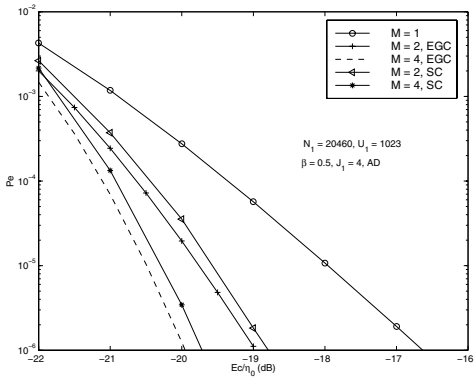

Figure 4: Probability of incorrect decision, P_e, versus E_c/η_0 performance of single-carrier ($M = 1$) and multicarrier ($M = 2, 4$) DS-SS with EGC and SC. Alternate data (AD).

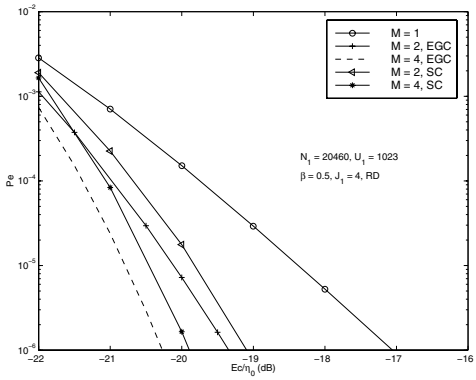

Figure 5: Probability of incorrect decision, P_e, versus E_c/η_0 performance of single-carrier ($M = 1$) and multicarrier ($M = 2, 4$) DS-SS with EGC and SC. Random data (RD).

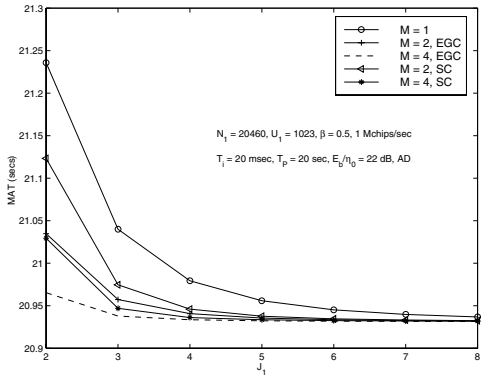

Figure 6: Mean acquisition time for the multicarrier DS-SS acquisition system for alternate data (AD) case.

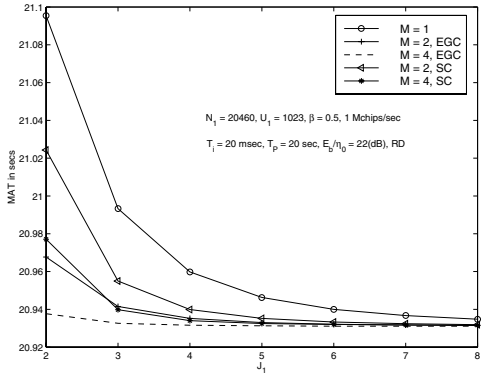

Figure 7: Mean acquisition time for the multicarrier DS-SS acquisition system for random data (RD) case.